Electronic Supplementary Material (ESI) for Journal of Materials Chemistry C.

Supplementary Information

Effects of line defects on the electronic and optical properties in strain-engineered WO_3 thin films

*Jing-ting Yang,[a,b,‡] Chao Ma,a,[‡] Chen Ge,[*a] Qinghua Zhang,[a] Jianyu Du,[a] Jiankun Li,[a] Heyi Huang,[a] Meng He,[a] Can Wang,[a] Sheng Meng,[a,c] Lin Gu,[a,b,c] Huibin Lyu,[a] Guozhen Yang[a,b,c] and Kuijuan Jin[*a,b,c]*

a Beijing National Laboratory for Condensed Matter Physics, Institute of Physics, Chinese Academy of Sciences, Beijing 100190, China

b School of Physical Sciences, University of Chinese Academy of Science, Beijing 100049, China

c Collaborative Innovation Center of Quantum Matter, Beijing 100871, China

‡ These authors contributed equally to this work.

*Corresponding Author: Chen Ge, gechen@iphy.ac.cn; Kuijuan Jin, kjjin@iphy.ac.cn

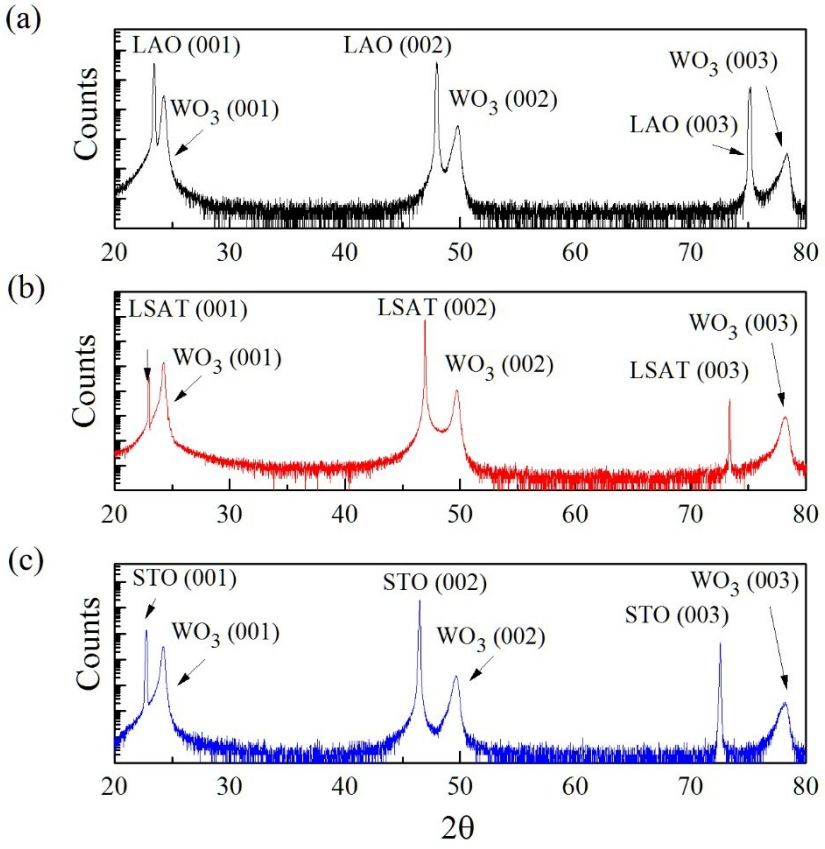

Fig. S1 (a-c) The XRD *θ-2θ* scanning curves of 50 nm thick WO_3 thin films grown on LAO (a), LSAT (b), and STO (c).

According to Fig. S1, the out-of-plane lattice constants are 3.660 Å, 3.665 Å and 3.669 Å for 50 nm thick WO_3 films grown on LAO, LSAT, and STO, respectively.

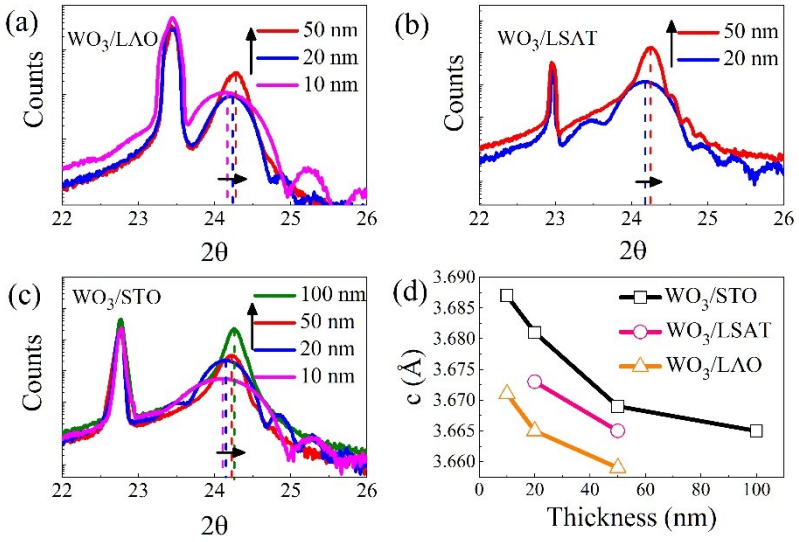

Fig. S2 (a-c) The XRD patterns of WO_3 thin films grown on LAO (a), LSAT (b), and STO (c) substrates with different thickness. (d) Out-of-plane lattice parameters of WO_3 vary with the film thickness for three substrates.

Fig. S2 (a-c) show the XRD θ-2θ scans of WO_3 with different thickness grown on LAO, LSAT and STO substrates, respectively. The (001) peaks of films grown on these three substrates all slightly shift toward right with increasing thickness, indicating smaller out-of-plane parameters in the thicker films as shown in Fig. S2 (d).

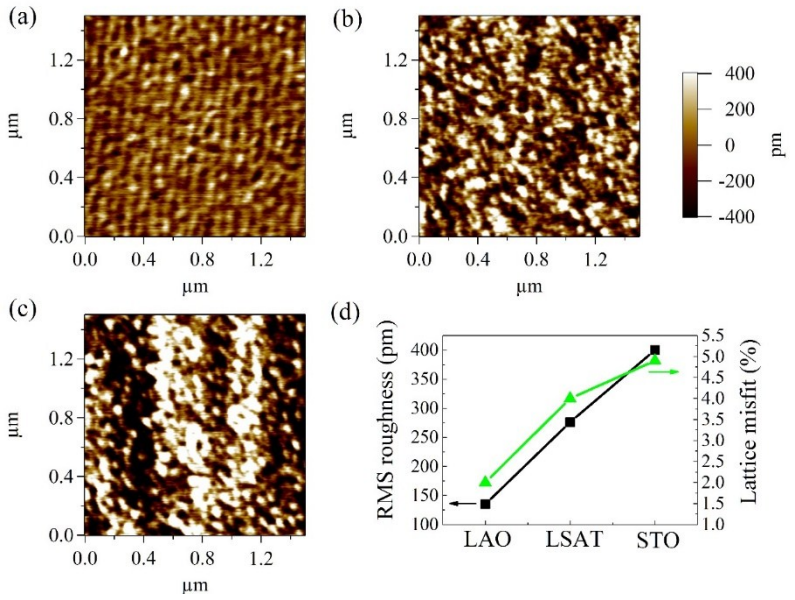

Fig. S3 AFM images of 20 nm thick WO_3 films grown on (a) LAO (001), (b) LSAT (001), and (c) STO (001). (d) The root-mean-square roughnesses and lattice mismatch of thin films with different substrates.

Fig. S3 is the AFM images with size of 1.5 ×1.5 μm^2 for 20 nm thick WO_3 films grown on (a) LAO (001), (b) LSAT (001), and (c) STO (001). The root-mean-square (rms) roughnesses are 135, 276 and 400 pm for LAO, LSAT, and STO, respectively. The small roughnesses indicate that all these films grow with atomically flat surfaces. With an increasing lattice mismatch between film and substrate, the surface of film become more roughly.

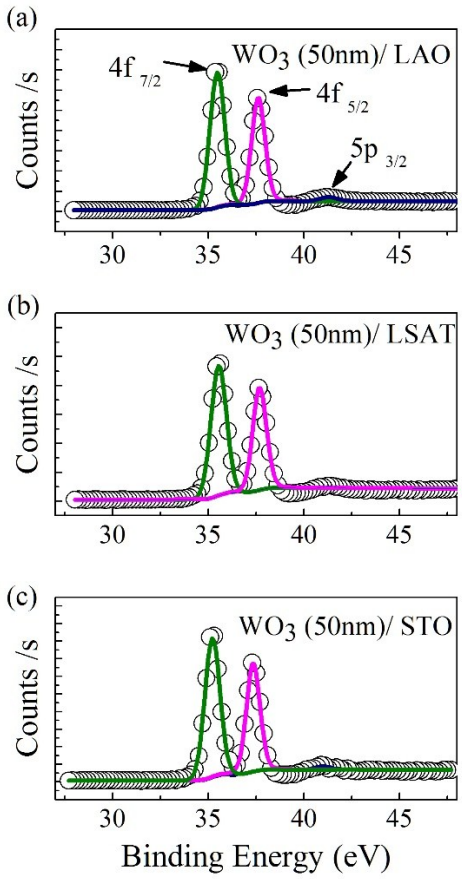

Fig. S4 XPS-spectrums of W 4f and 5p peaks for WO_3 epitaxial films on LAO (a), LSAT (b), and STO (c) substrates. Black symbols are the original data for XPS, and the olive, magenta, navy fitting lines correspond to W $4f_{7/2}$, $4f_{5/2}$, and $5p_{3/2}$ peaks, respectively.

The chemical states of tungsten atoms for the as-deposited 50 nm thick WO_3 films grown on different substrates were evaluated by XPS as shown in Fig. S4. The black symbols are the original data of XPS. The background signals is subtracted by Shirley method. The olive, magenta, navy lines are the fitting curves corresponding to W $4f_{7/2}$, $4f_{5/2}$, and $5p_{3/2}$ peaks, respectively. Referenced against C 1s at 284.6 eV, and the binding energies of the W $4f_{7/2}$ and W $4f_{5/2}$ lines have been found at 35.3-35.6 eV and

37.4-37.7 eV, respectively. The parameters of W 4f spin-orbit separation ΔE ($4f_{5/2}$ -$4f_{7/2}$) in all films are all 2.14 eV, with intensities ratios $I_{4f5/2}/I_{4f7/2} = 0.73 \pm 0.1$ eV. These characters of W 4f correspond with WO_3 in the earlier reports, [S1-S4] which indicating the existence of W^{6+} at the surface in each samples.

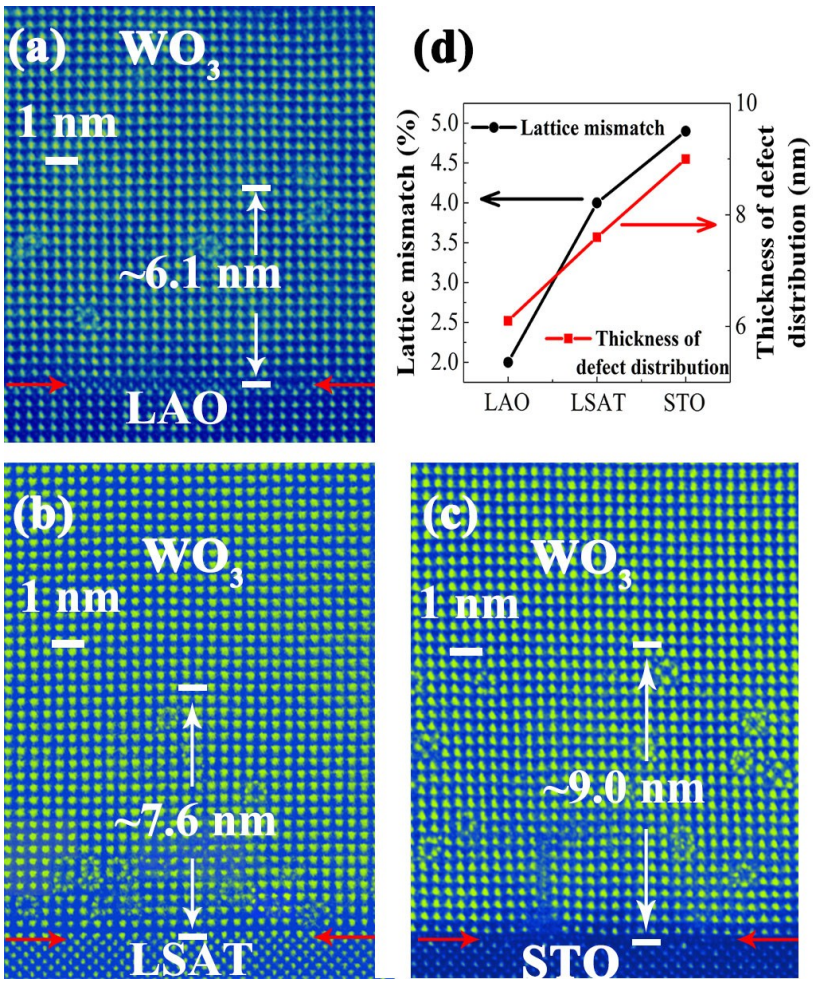

Fig. S5 STEM images of WO_3 films grown on (a) LAO, and (b) LSAT, (c) STO substrates viewed along the [100] direction. (d) The lattice mismatch (black symbol) and thickness of line defects distribution (red symbol) of thin films grown on different substrates.

Fig. S5 shows the spatial distribution of line defects in WO_3 thin films. Fig. S5 (a-c) revealed that line defects distribute only within ~6 nm away from the WO_3/LAO interface, ~7.6 nm away from the WO_3/LSAT interface, and ~9 nm away from WO_3/STO interface. With larger lattice mismatch, WO_3 thin films have more line defects distributing in thicker region away from interface.

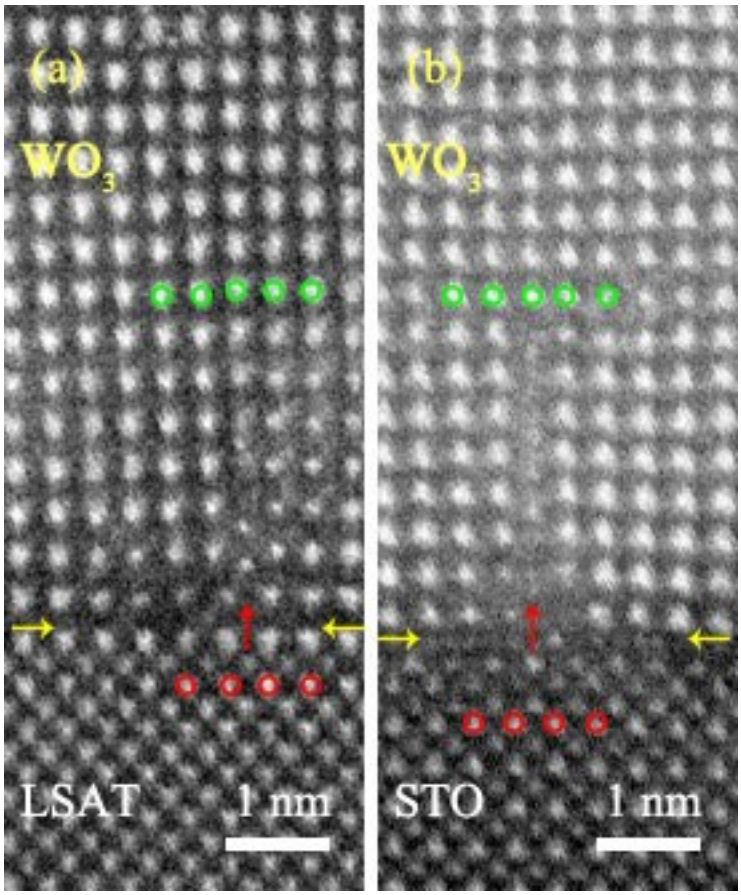

Fig. S6 Planar defects at the interface of film grown on (a) LSAT and (b) STO substrates revealed by STEM.

Fig. S6 shows the planar defect appearing at interface of WO_3/LSAT and WO_3/STO by STEM. These planar defects are in agreement with the recent report by Du *et al.* in WO_3/STO thin films.[S5] Yellow arrows indicate the position of epitaxial interface. Red circles indicate Al or Ta atoms in LSAT, and Ti atoms in STO. What's more, the green circles indicate W atoms. Four rows of W atoms are visible at the interface, compared to five rows of that in the same field of view further away from the interface. It looks like an intercalated column of tungsten atoms (marked by red arrow) in STEM image, which compresses adjacent column, and allows smaller in-plane constants of adjacent

WO_3 to accommodate near the interfaces. Actually, the planar defects make the tensile strain releasing gradually, and propagate the lattice distortion deeply into the film.

The existence of the line defects and the planar defects can explain why the out-of-plane lattice constant decreases with increasing film thickness (Fig. S2d). It is owing to the line defects and planar defects, which both compress adjacent WO_3 lattice and stretch their out-of-plane lattice constants near the interface. Hence, the existence of defects observed in the atomic scale is highly consistent with our XRD measurement.

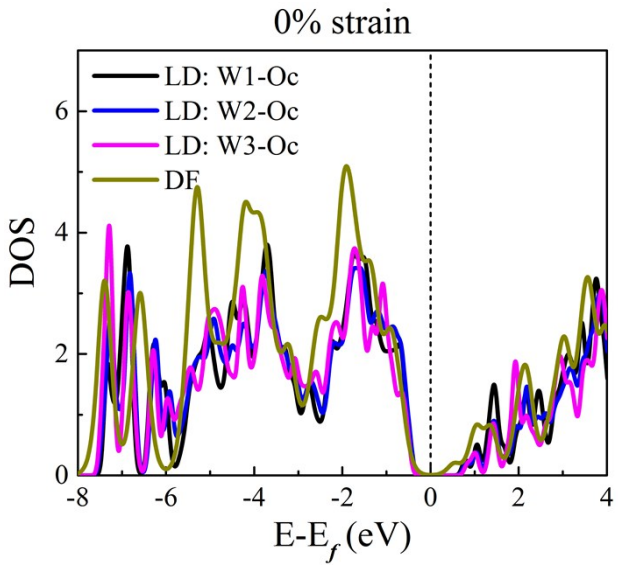

Fig. S7 The smoothing of the DOS while introducing line defects. The definition of "W*i*" is the same as that in Fig. 3a in the manuscript. Compared to the defective unit cells, the DOS of the defective-free unit cell has more remarkable peaks, especially around -2 eV, -4 eV, and -5.5 eV.

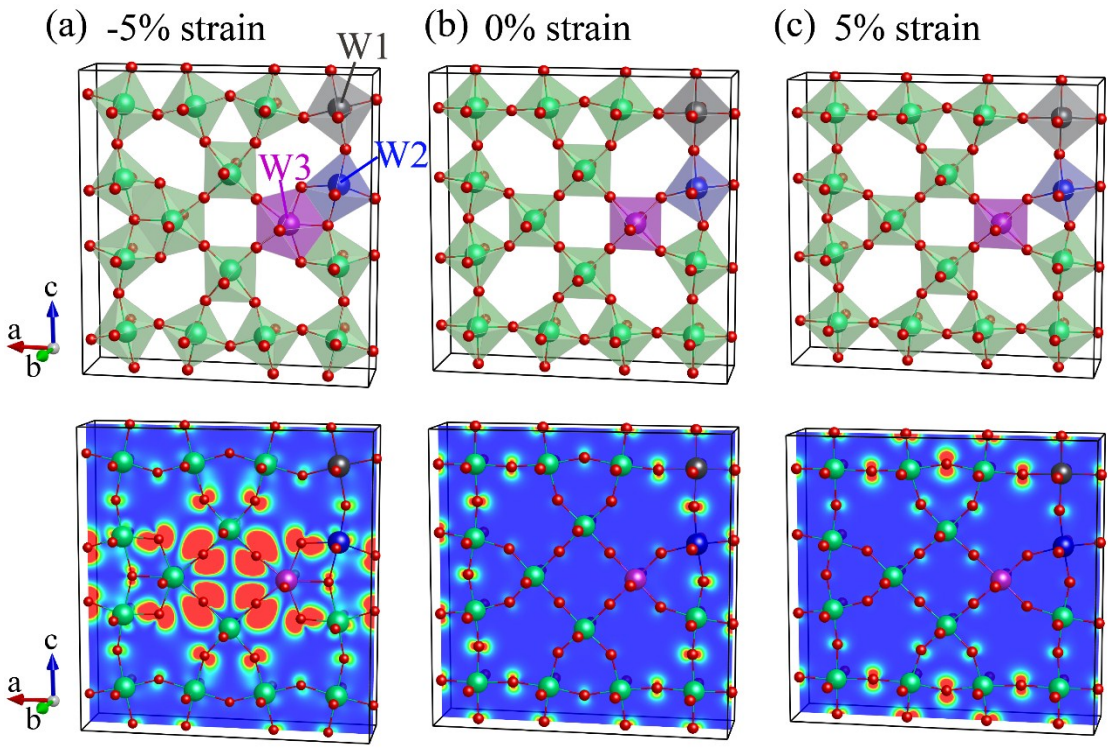

Fig. S8 The lattice structures (upper panels) and corresponding 2D-contourmaps of charge density distributions of the highest occupied band in the (0,2,0) plane (lower panels). The definition of "W*i*" and the contour levels (in B-G-R scale in all three contourmaps) are the same as that in fig. 3 in the manuscript. The charge distribution in (a) is much localized around the line defect at the center, which is in sharp contrast to that in (b) and (c). In addition, the W3 becomes 7-coordinated by oxygen atoms, the corresponding WO_6-octahedron therefore deforms to a WO_7-decahedron.

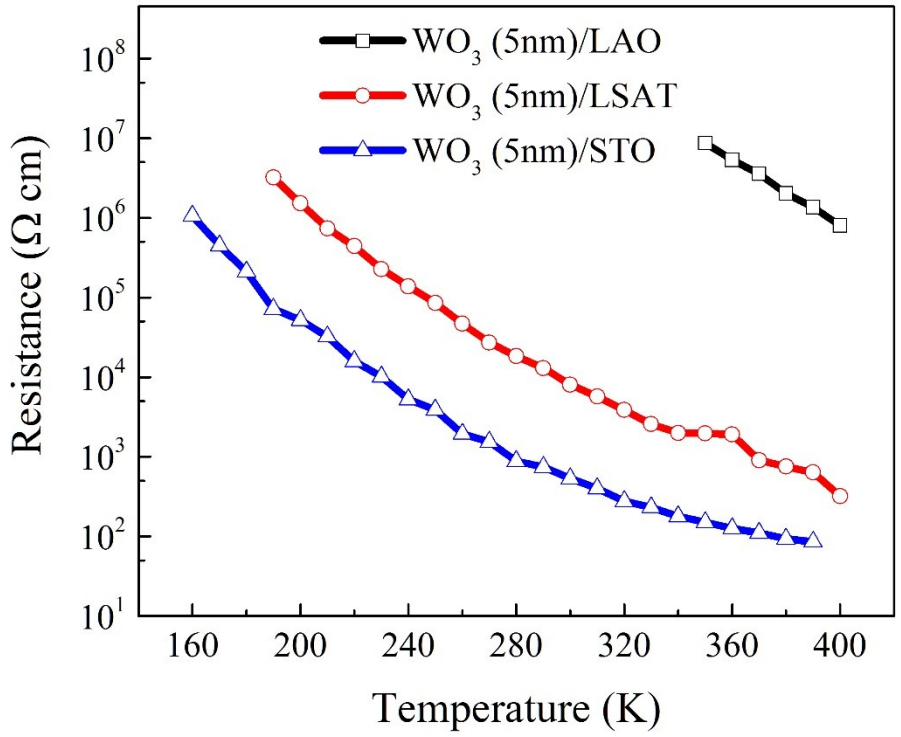

Fig. S9 Transport properties of 5 nm thick WO_3 grown on three different substrates. The resistance of thin films decreases with a larger tensile strain.

References

S1 T. H. Fleisch, G. J. Mains, *J. Chem. Phys.*, 1982, **76**, 780.

S2 P. Charton, L. Gengembre, P. Armand, *J. Solid State Chem.*, 2002, **168**, 175.

S3 A. P. Shpak, A. M. Korduban, M. M. Medvedskij, V. O. Kandyba, *J. Electron. Spectrosc. Relat. Phenom.*, 2007, **156**, 172.

S4 R. Azimirad, N. Naseri, O. Akhavan, A. Z. Moshfegh, *J. Phys. D: Appl. Phys.*, 2007, **40**, 1134.

S5 Y. Du, M. Gu, T. Varga, C. Wang, M. E. Bowden, S. A. Chambers, *ACS Appl. Mater. Interfaces*, 2014, **6**, 14253.